Dyes and Pigments 91 (2011) 356–363

Contents lists available at ScienceDirect

Dyes and Pigments

journal homepage: www.elsevier.com/locate/dyepig

A solution-processable deep red molecular emitter for non-doped organic red-light-emitting diodes

Zhiming Wang, Ping Lu*, Shanfeng Xue, Cheng Gu, Ying Lv, Qing Zhu, Huan Wang, Yuguang Ma*

State Key Laboratory of Supramolecular Structure and Materials, Jilin University, 2699 Qianjin Avenue, Changchun 130012, PR China

ARTICLE INFO

Article history:
Received 31 January 2011
Received in revised form
30 March 2011
Accepted 31 March 2011
Available online 28 April 2011

Keywords:
Solution-processable
Deep red emitter
Peripheral carbazole groups
Non-doped
OLEDs
Benzothiadiazole

ABSTRACT

A new solution-processable deep red emitter, **TCTzC**, containing dithienylbenzothiadiazole unit and four alkyl-linked peripheral carbazole groups, is designed and synthesized in high yield by Suzuki coupling reaction. The four peripheral carbazole substituents enhance the hole-transport ability, glass transition temperature, decompose temperature and film forming ability of **TCTzC**. The single-layered device based on **TCTzC** shows saturated deep red electroluminescence with a CIE coordinate of (0.70, 0.30). The current efficiency and quantum efficiency of **TCTzC** is two times higher than the compound without the four peripheral carbazole groups. The higher device performance is obtained when TPBi is applied and the external quantum efficiency could reach to 0.93%.

1. Introduction

Solution-processable emissive compounds have attracted tremendous attentions during the past decades in organic light-emitting diodes (OLEDs) field [1–6]. With respect to their polymer counterparts, solution-processable small molecules present the advantage of precise chemical structures and better reproducibility of synthesis, which facilitates the establishment of structure-property relationship [7–9]. They offer the possibility of avoiding the troublesome high-precision mask alignment during vacuum deposition process. Based on the current development of OLED materials [4,10–12], the design and synthesis of efficient non-doped red emitter with facile synthesis and purification method, good processability, efficient electron injection/transport capability and saturated red emission still remains the key issue [13–17].

Recently, our group reported a series of solution-processable molecules containing an emissive rigid core and four alkyl-linked peripheral carbazole groups (Scheme 1a) [18–21]. The alkyl side chain increases the solubility and flexibility of the compound, while the peripheral groups and emissive core tune the properties such as emission color, hole and electron injection and transport properties. For example, **TCBzC** (Scheme 1b), which has a benzothiadiazole unit as the core, had shown highly efficient green emission in a multi-layered device with a CIE of (0.34, 0.62) [20]. The single-layered spin-coating device exhibited the maximum luminous efficiency of 5.7 cd A^{-1}, which is among the best values of reported solution-processed single-layered green OLEDs. These kinds of materials may achieve high PL efficiency, bipolar charge injection and transport, and high performance of solution-processable OLEDs.

Thus, we designed new dithienylbenzothiadiazole (**DBT**) unit to develop saturated deep red emission [16,22,23]. We prepared a new pure red-emitting soluble **DBT** derivative, **TCTzC**, in which **DBT** unit is applied to realize the red emission because of its more conjugated structure (Scheme 1c). For further exploring the effect of peripheral carbazole groups, the model compound **MOD**, which has the similar structure as **TCTzC** but without peripheral carbazole groups, was also prepared and studied [24]. Herein, we reported the synthesis and photoelectronic properties of red-emitting **TCTzC**. **TCTzC** shows enhanced thermodynamic stability, film forming ability and hole-transport ability compared with **MOD**. The external quantum efficiency of the single-layered device is two times higher than that of **MOD**, when TPBi is used as the electron injection layer, the external quantum efficiency can reach to 0.93%.

* Corresponding authors. Tel.: +86 431 85167057; fax: +86 431 85168480.
E-mail addresses: lup@jlu.edu.cn (P. Lu), ygma@jlu.edu.cn (Y. Ma).

0143-7208/$ – see front matter © 2011 Elsevier Ltd. All rights reserved.
doi:10.1016/j.dyepig.2011.03.034

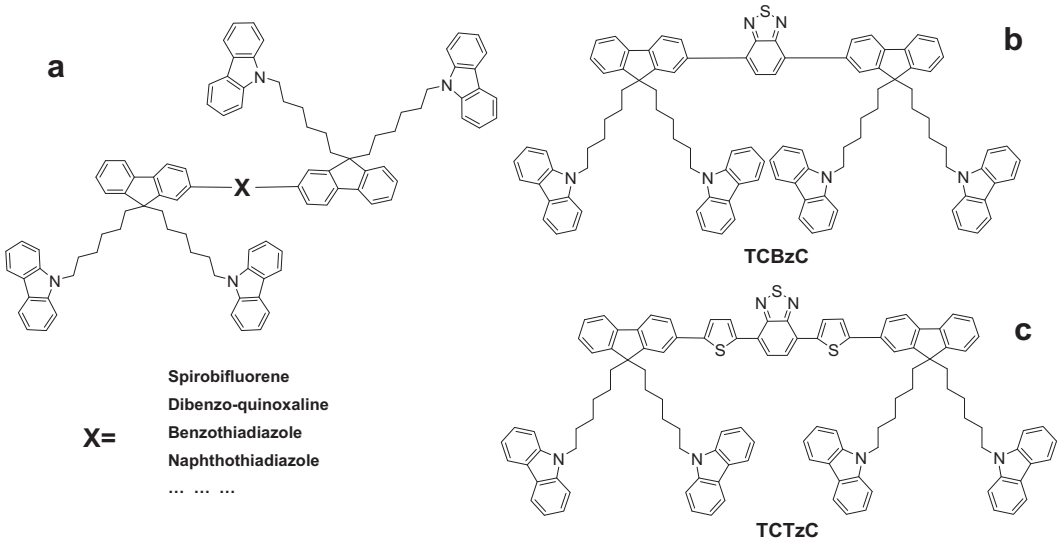

Scheme 1. The structures of a series of solution-processable small molecules (a) and the structures of **TCBzC** (b) and **TCTzC** (c).

2. Experimental part

2.1. Materials and measurement

All the reagents and solvents used for the synthesis were purchased from Aldrich or Acros companies and used without further purification. All reactions were performed under a dry nitrogen atmosphere.

The ^{1}H NMR and spectra were recorded on AVANCZ 500 spectrometers at 298 K by utilizing deuterated chloroform ($CDCl_3$) or dimethyl sulphoxide (DMSO) as solvent and tetramethylsilane (TMS) as standard. The elemental analysis was operated by Flash EA 1112, CHNS-O elemental analysis instrument. The MALDI-TOF mass spectra were recorded using an AXIMA-CFR™ plus instrument. Uv–vis absorption spectra were recorded on UV-3100 spectrophotometer. Fluorescence measurements were carried out with RF-5301PC. The differential scanning calorimeter (DSC) analysis was determined using a NETZSCH (DSC-204) instrument at 10 °C min^{-1} under nitrogen flushing. Cyclic voltammetry (CV) were performed with a BAS 100W Bioanalytical Systems, using a glass carbon disk (Φ = 3 mm) as working electrode, a platinum wire as auxiliary electrode and Ag/Ag$^+$ as reference electrode. Cyclic voltammetric studies were carried out containing 0.1 M [n-NBu_4][BF_4] supporting electrolyte. All solutions were purged with nitrogen stream for 10 min before measurement. The atomic force microscopy (AFM) measurement was conducted on a Nanoscope III (DI, USA) in tapping mode with 100 μm scanner.

2.2. OLEDs fabrication and measurement

The typical device configuration fabricated by spin-coating was ITO/PEDOT:PSS (40 nm)/**TCTzC** or **MOD**/LiF (0.5 nm)/Al (100 nm). The indium-tin-oxide (ITO)-coated glass with a sheet resistance of <50 s^{-1} was used as substrate. Pre-treatment of ITO included a routine chemical cleaning using detergent and alcohol in sequence, followed by oxygen plasma cleaning. The PEDOT:PSS (polyethylene dioxythiophene/polystyrene sulfonate) layer was spinned onto ITO-coated substrate. The **TCTzC** or **MOD** film was formed on PEDOT:PSS layer by spin-coating its chloroform solution with a concentration of 10 mg mL^{-1}. The electroluminescent (EL) spectra and Commission Internationale De L'Eclairage (CIE) coordination were measured by a PR650 spectroscan spectrometer. The luminance-current and density-voltage characteristics were recorded simultaneously with the measurement of the EL spectra by combining the spectrometer with a Keithley model 2400 programmable voltage-current source. All measurements were carried out at room temperature under ambient conditions.

2.3. Synthesis

2.3.1. 2-(thiophen-2-yl)-1,3,2-dioxaborinane (*M1*)

2-bromothiophene (7.79 g, 30.90 mmol) was dispersed in dry THF (100 mL) and added dropwisely into a 250 mL two-necked round-bottom flask containing Mg dust. Then it was refluxed until all the Mg dust dissolved. And then, it was transferred to the solution of trimethyl borate in dry THF at −78 °C. The mixture was stirred for 15 min at −78 °C and then warmed to room temperature for 30 min. Ice hydrochloric acid (10%) was poured into the mixture to stop the reaction. The organic layer was extracted with CH_2Cl_2 and dried with 4 Å molecular sieve for 12 h. After that, the solvent was removed under reduced pressure. The crude product was recrystallized from ethanol and yielded colorless crystals.

Yield: 80%. ^{1}H NMR ($CDCl_3$, ppm), δ: 7.56 (d, J = 4.8 Hz, 1H), 7.55 (d, J = 3.7 Hz, 1H), 7.16 (t, J = 4.8, 3.7 Hz, 1H), 4.16 (t, J = 5.1, 5.8 Hz, 4H), 2.07 (qui, J = 5.1, 5.8, 2H).

2.3.2. 4,7-di(thiophen-2-yl)benzo[c][1,2,5]thiadiazole (*M5*)

A mixture of **M1** (1.68 g, 10 mmol), **M2** (1.32 g, 4.5 mmol), K_2CO_3 (3.3 g, 12 mmol), water (6 mL) and toluene (30 mL) was refluxed under N_2 for 48 h. After cooling down to room temperature, the reaction mixture was poured into cool water and extracted with CH_2Cl_2 three times. The crude product was purified by silica-gel column chromatography using petroleum ether/CH_2Cl_2 (v:v = 4:1) as eluent to afford an orange solid.

Yield: 85%. ^{1}H NMR ($CDCl_3$, ppm), δ: 8.13 (d, J = 3.6, 1.2 Hz, 2H), 7.89 (s, 2H), 7.47 (d, J = 5.1, 1.2 Hz, 2H), 7.22(t, J = 5.1, 3.6, 1.2 Hz, 2H).

2.3.3. 4,7-bis(5-bromothiophen-2-yl)benzo[c][1,2,5]thiadiazole (*M6*)

A mixture of **M5** (1.5 g, 5 mmol), dichloromethane (10 mL) and DMF (20 mL) was stirred under a nitrogen flow in ice-water bath. After the solid dissolved completely, N-bromosuccinimide(NBS, 2.2 g, 12 mmol)/DMF (20 mL) was added droply. The reaction mixture was stirred at room temperature overnight under darkness. After that, the

formed deep red precipitate was filtered off, and the mixture was recrystallized from DMF to afford the deep red crystals of **M6**.

Yield: 65%. ^{1}H NMR (500 MHz) (d_6-DMSO) δ: 8.17 (s, 2H), 7.98 (d, J = 3.9, 2H), 7.41 (d, J = 3.9, 2H).

*2.3.4. 9,9′-(6,6′-(2-boron-9H-fluorene-9,9-diyl)bis(hexane-6,1-diyl))bis (9H-carbazole) (**M8**)*

Bis(pinacolato)diboron (0.28 g, 1.1 mmol), Pd(dppf)$_2$Cl$_2$ (30 mg, 0.03 mmol, 3%) and potassium acetate (0.3 g, 3.0 mmol) were put into a two-neck round-bottom flask equipped with a stirrer bar and reflux condenser. Then DMSO (8 mL) was added, and the mixture was stirred under nitrogen for 10 min. After that **M4** (0.74 g, 1.0 mmol) was added. The mixture was kept at 80 °C for 24 h. And then it was cooled down and extracted with CH_2Cl_2. The crude product was purified by silica-gel column chromatography using petroleum ether/CH_2Cl_2 (1:1, v/v) as eluent to afford a colorless solid.

Yield: 80%. ^{1}H NMR (500 MHz, $CDCl_3$, δ): 8.07-8.06 (d, J = 7.3 Hz, 4H), 7.82-7.80 (d, J = 7.3 Hz, 1H), 7.71-7.68 (m, 3H), 7.44-7.40 (m, 4H), 7.32-7.27 (m, 5H), 7.24-7.23 (d, J = 5.5 Hz, 2H), 7.22-7.28 (m, 4H), 4.16-4.13 (m, 4H), 1.97-1.86 (m, 4H), 1.68-1.62 (m, 4H), 1.36 (s, 12H), 1.15-1.00 (m, 8H), 0.61-1.47 (m, 4H).

*2.3.5. Synthesis of **TCTzC***

TCTzC was synthesized by Suzuki coupling reaction using Pd(PPh$_3$)$_4$ as the catalyst. The reaction mixture of M6 (0.2 mmol) and M7 (0.45 mmol) were stirred at 90 °C for 2 days under a nitrogen atmosphere, respectively. The reaction was stopped by water, and the mixture was extracted three times with chloroform. The organic phase was then dried over anhydrous magnesium sulfate. After filtration and rotary evaporation, the liquid was purified by column chromatography using petroleum ether/CH_2Cl_2 (10:1, v/v) as the eluent to afford a deep-red solid.

Yield: 70%. ^{1}H NMR (500 MHz, DMSO-d$_6$, δ): 8.23 (s, 2H), 8.16 (s, 2H), 8.11-8.04 (d, J = 7.6 Hz, 8H), 7.86-7.82 (d, J = 8.2 Hz, 2H), 7.81-7.62 (m, 4H), 7.60-7.10 (m, 4H), 7.49-7.41 (d, J = 8.2 Hz, 8H), 7.40-7.33 (t, J = 7.3, 7.0 Hz, 8H), 7.32-7.21 (m, 8H), 7.16-7.06 (t, J = 8.2, 7.0 Hz, 8H), 4.28-4.18 (t, J = 7.6, 7.3 Hz, 8H), 2.06-1.84 (m, 8H), 1.55-1.53 (m, 8H), 1.10-0.95 (m, 8H), 0.91-0.72(m, 8H), 0.58-0.46 (m, 8H). ^{13}C NMR (125 MHz, $CDCl_3$, ppm): 153.0, 151.7, 150.9, 146.8 (carbazole group), 141.5, 140.9, 140.7(carbazole group), 138.8, 133.4, 129.0, 127.8, 127.4, 126.2, 125.9 (carbazole group), 125.7, 125.3, 124.4, 123.1, 120.7, 120.3, 119.0 (carbazole group), 109.0 (carbazole group), 55.7, 43.3, 40.7, 30.4, 29.1, 27.2, 23.9. MALDI-TOF-MS (m/z): [M + H]$^+$Calcd for $C_{112}H_{100}N_6S_3$: 1625.2; Found:1625.1. Anal. Calcd. for $C_{112}H_{100}N_6S_3$: C, 82.72; H, 6.20; N, 5.17; S, 5.92; Found: C, 82.55; H, 6.18; N, 5.18.

*2.3.6. Synthesis of **MOD***

MOD was synthesized with the same procedure as **TCTzC**. Yield: 60%. ^{1}H NMR (500 MHz, DMSO-d_6, δ): 8.28-8.25 (d, J = 3.7 Hz, 2H), 8.22 (s, 2H), 7.92-7.88 (d, J = 8.2 Hz, 2H), 7.88-7.83 (m, 4H), 7.82-7.76 (m, 4H), 7.50-7.45 (m, 2H), 7.40-7.33 (m, 4H), 2.06-1.99 (m, 8H), 1.13-0.95 (m, 16H), 0.92-0.80 (m, 8H), 0.78-0.65 (m, 8H), 0.62-0.45 (m, 12H). ^{13}C NMR (125 MHz, $CDCl_3$, ppm): 153.1, 152.0, 151.4, 141.6, 140.9, 138.7, 133.3, 129.1, 127.7, 127.3, 126.3, 125.7, 125.2, 124.3, 123.3, 120.5, 120.2, 55.7, 40.8, 31.9, 30.1, 24.2, 22.9, 14.4. MALDI-TOF-MS (m/z): [M + H]$^+$Calcd for $C_{64}H_{72}N_2S_3$: 964.4; Found: 965.1. Anal. Calcd. for $C_{64}H_{72}N_2S_3$: C, 79.62; H, 7.52; N, 2.90; S, 9.96; Found: C, 79.54; H, 7.54; N, 2.91.

3. Results and discussion

3.1. Design and synthesis

The synthetic details are shown in Scheme 2. The thiophenboronic ester (**M1**) was synthesized by Grignard reagent method using bromothiophen as the starting material [25]. This method shows a higher yield than the traditional one using *n*-butyllithium reagents [26,27]. **M2**, **M3**, **M4** and **M7** were prepared according to our published procedures [18,28–30]. **M5** was synthesized by Suzuki coupling reaction between **M1** and **M2** with a high yield of 85%. **M6** was prepared by bromonation of **M5** with NBS under darkness with a nearly 70% yield. The hydrogen at the 3,6-position of carbazole in **M4** was not stable when *n*-butyllithium was added, and the yield of **M8** was only 5%. To improve the yield, **M4** was first reacted with bis(pinacolato)diboron in the presence of palladium catalyst and potassium acetate, and thus the yield of **M8** could be increased to 80% [30–33].

TCTzC and **MOD** were prepared by Suzuki coupling reaction between the monomers of **M6** or **M7** with **M8**, respectively. The products were purified by chromatography using petroleum ether/CH_2Cl_2 as eluent. The structures of target products, **TCTzC** and **MOD**, were confirmed by ^{1}H NMR, ^{13}C NMR, MALDI-TOF mass measurement and corresponded well with their respected structures. They both showed good solubility in common organic solvents such as dichloromethane, tetrahydrofuran and toluene.

3.2. Structure analysis

Fig. 1 shows the ^{1}H NMR spectra of **TCTzC** and **MOD** in the aromatic range. Because the two oligomers have the same backbone, the similar chemical shift and peak shapes are observed. The resonances that appeared at 8.09(a), 7.43(d), 7.33(b) and 7.13(c)

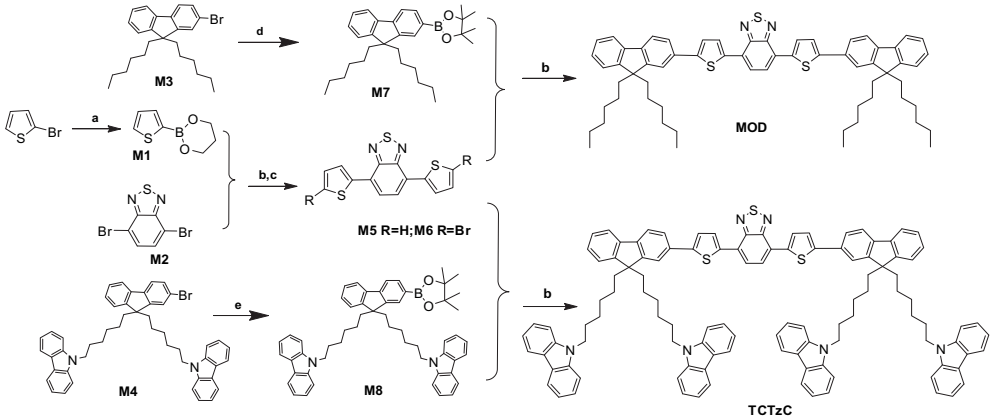

Scheme 2. The synthetic route to **TCTzC** and **MOD**. (a. Mg dust, trimethyl borate, in THF at −78 °C; b. K_2CO_3, water, toluene, refluxed, 48 h; c. dichloromethane, DMF, NBS, ice-water bath; d, n-BuLi, (pinacolato)diboron, in THF at −78 °C; e, Bis(pinacolato)diboron, Pd(dppf)$_2$Cl$_2$, potassium acetate, DMSO, 80 °C, 24 h.

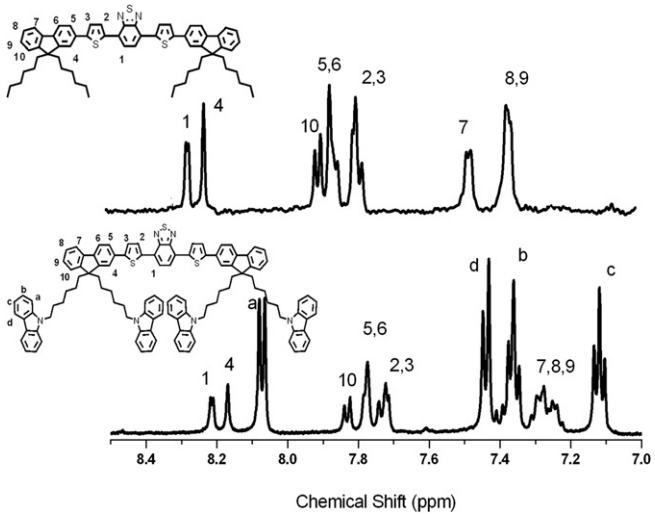

Fig. 1. ^{1}H NMR spectra of **TCTzC** and **MOD** in the aromatic range.

correspond to the protons resonance of the four peripheral carbazole groups [18,20].

3.3. Photophysical properties

The Uv–vis absorption spectra of **TCTzC** and **MOD** in dilute tetrahydrofuran (THF) solution and in film state are shown in Fig. 2a and c, and the relevant data are summarized in Table 1. The absorption spectrum of **MOD** in THF solution has two absorption bands peaking at 365 and 510 nm, respectively. The absorption band around 365 nm, is attributed to $\pi-\pi^*$ electronic transitions in the fluorene backbone [18], which is similar to that observed for reported fluorene-based oligomers. The low-energy band around 510 nm is attributed to the absorption of the **DBT** unit incorporated into the polyfluorene chain (a low energy intramolecular charge transfer transition) [34,35]. In **TCTzC**, besides the two bands, three new high-energy sharp absorption peaks at 260, 291 and 344 nm are observed which are attributed to transitions of the peripheral carbazole groups [18].

The absorption spectra of **TCTzC** and **MOD** in film state show similar characteristics as those in THF solution but with a large red-shift, which might be from the strong $\pi-\pi^*$ intramolecular interactions (Fig. 2c). λ_{onset} of two oligomers are both at 800 nm, thus the band gaps are both calculated to be 1.55 eV.

In THF solution, both of them exhibit very strong deep-red fluorescence upon excitation at 365 nm (Shown in Fig. 2b). Emission maximum (λ_{max}) is observed at 618 nm for **MOD** and 622 nm for **TCTzC**, which derives from the intramolecular charge transfer. The emission of the fluorene unit is completely disappeared in **TCTzC** and PL emission came exclusively from **DBT** unit [34]. The CT character of the excited state is further evidenced by the shift of the λ_{max} in solvents with different polarity. For instance, λ_{max} of **TCTzC** is at 587 nm in hexane, 603 nm in toluene, 622 nm in THF, and 648 nm in CH_3CN, respectively [36,37]. When **TCTzC** is excited at 291 nm or 344 nm, no emission from the peripheral carbazole groups is observed, indicating efficient intramolecular energy transfer from the carbazole groups to the backbone of **TCTzC** [18]. The quantum yield of **TCTzC** is 0.32 in THF using Rhodamine B in

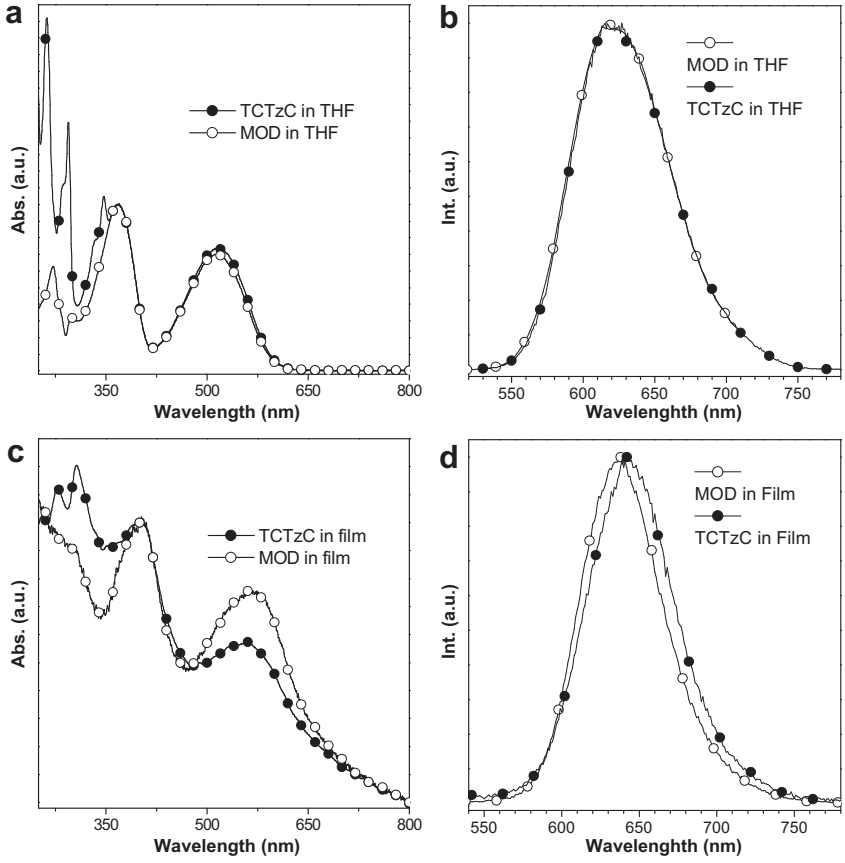

Fig. 2. Uv–vis absorption (a,c) and fluorescence (b,d) spectra of **TCTzC** and **MOD** in THF and film.

Table 1
The thermal, photophysical and electrochemistry data of **MOD** and **TCTzC**.

	T_g (°C)	T_d (°C)	Abs in THF (nm)[a]	PL (nm)[b]				HOMO (eV)[c]	LUMO (eV)[c]	Eg (eV)[c]
				Hexane	Toluene	THF	CH_3CN			
MOD	54	450	365, 510	585	607	618	623	−5.30	−3.31	1.99
TCTzC	90	486	260, 291, 344, 365, 510	587	603	622	648	−5.24	−3.30	1.94

[a] Measured in THF (10^{-5} M).
[b] Measured in solution (10^{-5} M).
[c] Calculated by comparing with ferrocene (Fc) (4.8 eV).

ethanol as the reference ($\Phi = 0.64$). In film state, **MOD** and **TCTzC** both show red-shift compared to their solutions which is from the strong π−π* intramolecular interactions. The λ_{max} is at 637 nm for **MOD** and 643 nm for **TCTzC** [6]. Meanwhile, the quantum efficiency of **TCTzC** in film is decreased to 0.17.

3.4. Thermal properties

The thermal properties of **TCTzC** and **MOD** are investigated by thermogravimetric analysis (TGA) and differential scanning calorimetry (DSC). As shown in Fig. 3 a, TGA spectra both show two-step thermal decomposition process, and the 10% loss of weight is measured to be 450 °C for **MOD** and 482 °C for **TCTzC**. Differential scanning calorimetry (DSC) measurement of **TCTzC** shows a distinct glass transition at 90 °C in the second heating run. This value represents a marked improvement compared to the T_g of 54 °C for **MOD** (shown in Fig. 3b). Neither crystallization nor melting peak is observed upon heating until 300 °C. The improved T_g of **TCTzC** originates from the carbazole groups attached to the side chain of the fluorene. The π−π* interaction between carbazole units is like an anchor which increases the intermolecular twisted degree and movement barrier [38,39]. From TGA and DSC analysis, **TCTzC** shows higher thermal stability, which is very important for the OLEDs application.

3.5. Electrochemical properties

To compare the electrochemical properties of **TCTzC** and **MOD**, cyclic voltammetry (CV) measurements are performed in a three-electrode cell using 0.1 M *n*-Bu_4NBF_4 as the supporting electrolyte and ferrocene (Fc) as the internal standard. In oxidation progress, three peaks are observed in **TCTzC**, while the **MOD** shows only two peaks. New oxidation peak is observed at 0.88 V in **TCTzC**, which is ascribed to the oxidation of the carbazole units (Fig. 4). This is consistent with results reported in the literature for the electrochemical behavior of carbazole and its derivatives [19,20]. The highest occupied molecular orbital (HOMO) energy levels are calculated to be −5.24 eV for **TCTzC** and −5.30 eV for **MOD**. The HOMO energy levels of both compounds approach the work function of poly(3,4-ethylenedioxythiophene) (PEDOT, −5.2 eV). In reduction progress, the quasi-reversible redox peaks are both observed at about 1.41 V, because the same reduction process occurred on the **DBT** unit [21]. The LUMO energy levels are calculated both to be −3.30 eV for **TCTzC** and **MOD**.

In previous report of the **DBT**-based OLEDs, they often showed good electron injection ability. To get the balanced carrier injection and transport property, it was often doped with different host materials such as PFO, PVK and MEH-PPV. Although the OLED showed high performance, the emission color relied on the doped concentration and the color purity was not good. In addition, it increased the cost and flexibility of the device. The introduction of carbazole units might solve the problem. Enhanced hole injection ability and balanced the carries injection and transport property could be expected in **TCTzC** [22,23,34].

3.6. Morphology properties

TCTzC and **MOD** both could form continuous amorphous films when spin-coated from $CHCl_3$ solution (Fig. 5c and d). The atomic force microscopy (AFM) image of **TCTzC** film shows a roughness value of 5.7 nm, while **MOD** shows a roughness of 27.5 nm on naked ITO surface. In general, the crystallization could induce the molecular self-aggregation [40,41]. The result indicates the carbazole groups might disrupt intermolecular interactions and reduce self-aggregation because of bulky substituent [16]. We also measured the AFM images of spin-coated **TCTzC** film on

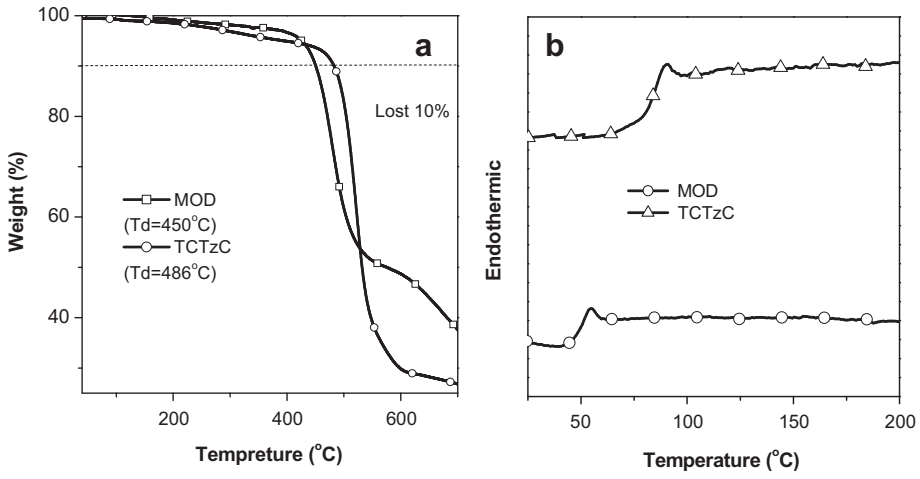

Fig. 3. The DSC (a) and TGA (b) spectra of **TCTzC** and **MOD**.

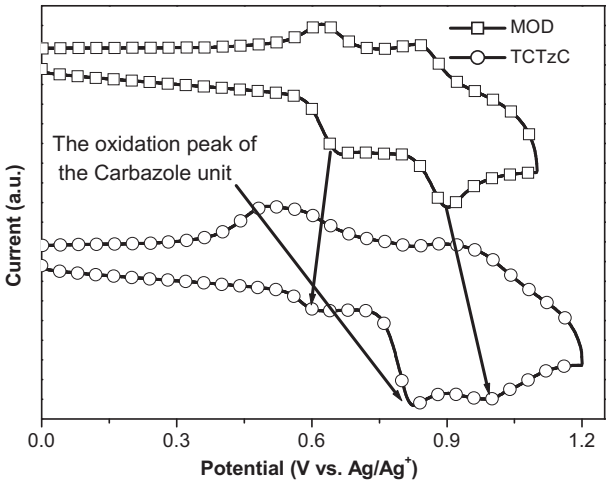

Fig. 4. CV curves of **TCTzC** and **MOD**.

a PEDOT:PSS layer, which shows a smooth and featureless morphology with a roughness less than 0.4 nm (Fig. 5a and b), which is very important for application in OLEDs.

3.7. Electroluminescent properties

The electroluminescent properties of solution-processed **TCTzC** is studied in a single-layered electroluminescent device with a configuration of ITO/PEDOT (80 nm)/**TCTzC** (45 nm)/LiF (0.5 nm)/Al (120 nm). The characteristics of the single-layered devices are summarized in Table 2. The device using **TCTzC** as the emission layer exhibits a maximum luminance efficiency of 0.10 cd A^{-1}, corresponding to an external quantum efficiency of 0.27%. In contrast, the single-layered device based on **MOD** shows

Table 2
The devices performance of **MOD** and **TCTzC**.

Device	CIE (x, y)	Voltage [V][c]	L_{max} [cd m^{-2}]	LE_{max} [cd A^{-1}]	EQE_{max} [%]
MOD[a]	(0.65, 0.33)	5.5	81	0.05	0.10
TCTzC[a]	(0.69, 0.31)	6.0	45	0.10	0.27
TCTzC[b]	(0.70, 0.30)	4.0	932	0.22	0.93

[a] The device structure: ITO/PEDOT (80 nm)/**TCTzC** or **MOD**/LiF (0.5 nm)/Al (120 nm).
[b] The device structure: ITO/PEDOT/**TCTzC**/TPBi (50 nm)/LiF (0.5 nm)/Al (100 nm).
[c] The turn-on voltage (L > 1 cd m^{-2}).

a maximum luminance efficiency of 0.05 cd A^{-1}, corresponding to an external quantum efficiency of 0.10%. The efficiency of **TCTzC** is as twice as that of **MOD**. This is possibly due to the introduction of carbazole groups which increases the hole injection and transport, resulting in a dramatic improvement of the EL performance of **TCTzC**. And the two compounds both exhibit deep and pure red emission, and λ_{max} is at 668 nm for **TCTzC** with a CIE of (0.69, 0.31), and 652 nm for **MOD** with a CIE of (0.65, 0.33), respectively. The emission is even beyond the PR650 detection range and some light longer than 780 nm could not be detected. Comparing to the emission peak in film state, the red shift in EL is observed, which is quite common in ICT-based materials.

To further improve the device efficiency, applying an electron-transporting layer between the emitting layer and the anode is tried. Device with a configuration of ITO/PEDOT/**TCTzC**/1,3,5-tris(*N*-phenylbenzimidazol-2-yl) benzene (TPBi)/LiF (0.5 nm)/Al (100 nm) has been fabricated, where TPBi acts as a hole-blocking layer and an electron-transporting layer to confine the carriers in the active layer. The device exhibits better performance with a maximum luminance of 932 cd m^{-2}, a maximum luminance efficiency of 0.22 cd A^{-1}, and an external quantum efficiency of 0.93% (Fig. 6a). The device exhibits deep-red emission with a CIE of (0.70 0.30), and

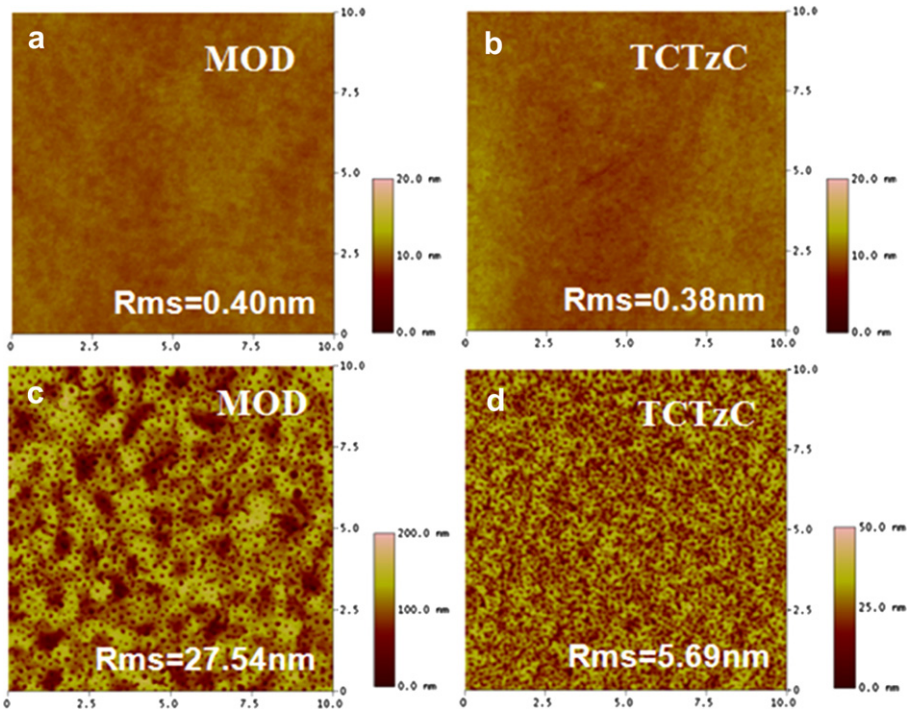

Fig. 5. AFM images of spin-coated **TCTzC** and **MOD** films at room temperature (a, b: on a PEDOT:PSS layer; c, d: on naked ITO).

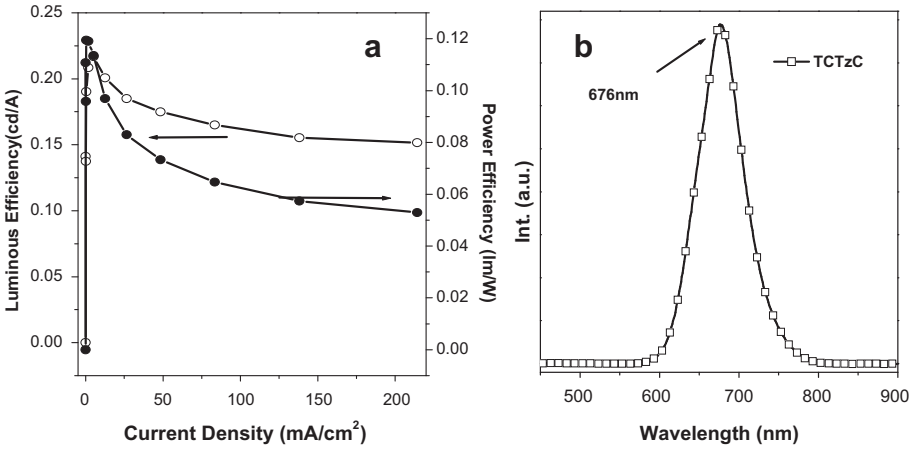

Fig. 6. (a) The device characteristics of **TCTzC** with the configuration of ITO/PEDOT/**TCTzC**/TPBi/LiF/Al, and (b) the EL spectra of **TCTzC**.

this EL efficiency is a good value for deep-red OLEDs) (Fig. 6b). Furthermore, the electroluminescence spectra of these compounds are stable with increasing voltage, and no other emission is observed.

4. Conclusions

In summary, a soluble red fluorescent molecular glass based on dithienylbenzothiadiazole, **TCTzC**, has been synthesized in high yield by Suzuki coupling reaction. The four peripheral carbazole substituents improve the hole injection ability, glass transition temperature, decompose temperature and the forming film ability. The single-layered OLED based on **TCTzC** shows deep red electroluminescence with two time higher efficiency than the one without peripheral carbazole groups. The external quantum efficiencies of a double-layered device could reach to 0.93%. Solution-processable saturated red emitter is got by our design strategy.

Acknowledgments

We are grateful for support from the National Science Foundation of China (Grant No. 20704016, 20834006), the Ministry of Education of China (Grant No.20070183202), the Ministry of Science and Technology of China (grant number: 2009CB623605) and PCSIRT.

References

[1] Lo SC, Burn PL. Development of dendrimers: macromolecules for use in organic light-emitting diodes and solar cells. Chem Rev 2007;107:1097–116, http://pubs.acs.org/doi/abs/10.1021/cr050136l.
[2] Luo J, Zhou Y, Niu ZQ, Zhou QF, Ma YG, Pei J. Three-dimensional architectures for highly stable pure blue emission. J Am Chem Soc 2007;129:11314–5, http://dx.doi.org/10.1021/ja073466r.
[3] Pu YJ, Higashidate M, Nakayama KI, Kido J. Solution-processable organic fluorescent dyes for multicolor emission in organic light emitting diodes. J Mater Chem 2008;18:4183–8, http://pubs.rsc.org/en/Content/ArticleLanding/2008/JM/b806160b.
[4] Zhou Y, He QQ, Yang Y, Zhong HZ, He C, Sang GY, et al. Binaphthyl-containing green- and red-emitting molecules for solution-processable organic light-emitting diodes. Adv Funct Mater 2008;18:3299–306, http://onlinelibrary.wiley.com/doi/10.1002/adfm.200800375/abstract.
[5] Choa MJ, Jina JI, Choia DH, Kimb YM, Park YW, Jub BK. Phosphorescent, green-emitting Ir(III) complexes with carbazolyl-substituted 2-phenylpyridine ligands: effect of binding mode of the carbazole group on photoluminescence and electrophosphorescence. Dyes Pigm 2009;83:218–24, http://dx.doi.org/10.1016/j.dyepig.2009.04.010.
[6] Huang J, Li C, Xia YJ, Zhu XH, Peng J, Cao Y. Amorphous fluorescent organic emitters for efficient solution-processed pure red electroluminescence: synthesis, purification, morphology, solid-state photoluminescence, and device characterizations. J Org Chem 2007;72:8580–3, http://pubs.acs.org/doi/abs/10.1021/jo7014517.
[7] Oldham WJ, Lachicotte RJ, Bazan GC. Synthesis, spectroscopy, and morphology of tetrastilbenoidmethanes. J Am Chem Soc 1998;120:2987–8, http://pubs.acs.org/doi/abs/10.1021/ja974209x.
[8] Robinson MR, Wang SJ, Bazan GC, Cao Y. Electroluminescence from well-defined tetrahedral oligophenylenevinylene tetramers. Adv Mater 2000;12:1701–4, http://dx.doi.org/10.1002/1521-4095(200011)12:22<1701::AID-ADMA1701>3.0.CO;2-U.
[9] Chen ACA, Culligan S, Geng YH, Chen SH, Klubek KPK, Vaeth M, et al. Organic polarized light-emitting diodes via förster energy transfer using monodisperse conjugated oligomers. Adv Mater 2004;16:783–8, http://dx.doi.org/10.1002/adma.200306265.
[10] Zhao L, Zou JH, Huang J, Li C, Zhang Y, Sun C, et al. Asymmetrically 9,10-disubstituted anthracenes as soluble and stable blue electroluminescent molecular glasses. Org Electron 2008;9:649–55, http://dx.doi.org/10.1016/j.orgel.2008.04.006.
[11] Sun YH, Zhu XH, Chen Z, Zhang Y, Cao Y. Potential solution processible phosphorescent iridium complexes toward applications in doped light-emitting diodes: rapid syntheses and optical and morphological characterizations. J Org Chem 2006;71:6281–4, http://pubs.acs.org/doi/abs/10.1021/jo060840h.
[12] Kulkarni AP, Tonzola CJ, Babel A, Jenekhe SA. Electron transport materials for organic light-emitting diodes. Chem Mater 2004;16:4556–73, http://pubs.acs.org/doi/abs/10.1021/cm049473l.
[13] Ho CL, Wong WY, Gao ZQ, Chen CH, Cheah KW, Yao BZ, et al. Red-light-emitting iridium complexes with hole-transporting 9-rrylcarbazole moieties for electrophosphorescence efficiency/color purity trade-off optimization. Adv Funct Mater 2008;18:319–31, http://onlinelibrary.wiley.com/doi/10.1002/adfm.200700665/abstract.
[14] Zhou GJ, Wong WY, Yao B, Xie ZY, Wang LX. Triphenylamine-dendronized pure red iridium phosphors with superior OLED efficiency/color purity trade-offs. Angew Chem Int Ed Engl 2007;46:1149–51, http://dx.doi.org/10.1002/anie.200604094.
[15] Barker CA, Zeng XS, Bettington S, Batsanov AS, Bryce MR, Beeby A. Porphyrin, phthalocyanine and porphyrazine derivatives with multifluorenyl substituents as efficient deep-red emitters. Chem Eur J 2007;13:6710–7, http://onlinelibrary.wiley.com/doi/10.1002/chem.200700054/abstract.
[16] Huang J, Liu Q, Zou JH, Zhu XH, Li AY, Li JW, et al. Electroluminescence and laser emission of soluble pure red fluorescent molecular glasses based on dithienylbenzothiadiazole. Adv Funct Mater 2009;19:2978–86, http://onlinelibrary.wiley.com/doi/10.1002/adfm.200900365/abstract.
[17] Cao XB, Wen YG, Guo YL, Yu G, Liu YQ, Yang LM. Undoped red organic light-emitting diodes based on a N, N, N′, N′-tetraphenylbenzidine (TPD) derivative as red emitter with a triphenylamine derivative as hole-transporting layer. Dyes Pigm 2010;84:203–7, http://dx.doi.org/10.1016/j.dyepig.2009.08.003.
[18] Tang S, Liu MR, Lu P, Gu C, Zeng M, Xie ZQ, et al. Fluorene trimers with various 9,9′-substituents: the synthesis, characteristics, condensed state structures, and electroluminescence properties. Org Electron 2008;9:241–52, http://dx.doi.org/10.1016/j.orgel.2007.10.010.
[19] Li M, Tang S, Shen FZ, Liu MR, Xie W, Xia H, et al. Highly luminescent network films from electrochemical deposition of peripheral carbazole functionalized fluorene oligomer and their applications for light-emitting diodes. Chem Commun 2006;32:3393–5, http://pubs.rsc.org/en/Content/ArticleLanding/2006/CC/b607242a.
[20] Zhang M, Xue SF, Fei T, Wang Q, Gu C, Ma YG. Highly efficient solution processed OLEDs based on new bipolar emitters. Chem Commun 2010;46:3923–5, http://pubs.rsc.org/en/Content/ArticleLanding/2010/CC/c001170c.
[21] Gu C, Fei T, Lv Y, Feng T, Xue SF, Lu D, et al. Color-stable white electroluminescence based on a cross-linked network film prepared by electrochemical

copolymerization. Adv Mater 2010;22:2702–5, http://onlinelibrary.wiley.com/doi/10.1002/adma.201000347/abstract.
[22] Luo J, Peng J, Cao Y, Hou Q. High-efficiency red light-emitting diodes based on polyfluorene copolymers with extremely low content of 4,7-di-2-thienyl-2,1,3- benzothiadiazole-comparative studies of intrachain and interchain interaction. Appl Phys Lett 2005;87:261103, http://apl.aip.org/resource/1/applab/v87/i26/p261103_s1 (3 p.ges).
[23] Niu YH, Hou Q, Cao Y. High-efficiency polymer light-emitting diodes with stable saturated red emission based on blends of dioctylfluorene-benzothiadiazole dithienylbenzothiadiazole terpolymers and poly [2-methoxy-2-ethylhexoxy-1,4-phenylene vinylene]. Appl Phys Lett 2003;82:2163–5, http://apl.aip.org/resource/1/applab/v82/i13/p2163_s1.
[24] Kim JH, Herguth P, Kang M, Tseng YH, Shu CF, Jen AK. Bright white light electroluminescent devices based on a dye-dispersed polyfluorene derivative. Appl Phys Lett 2005;85:1116, http://apl.aip.org/resource/1/applab/v85/i7/p1116_s1 (3 p.ges).
[25] Lu J, Xia P, Lo PK, Tao Y, Wong MS. Synthesis and properties of multitriarylamine-substituted carbazole-based dendrimers with an oligothiophene core for potential applications in organic solar cells and light-emitting diodes. Chem Mater 2006;18:6194–204, http://pubs.acs.org/doi/abs/10.1021/cm062111o.
[26] Labadie JW, Tueting J, Stille JK. Synthetic utility of the palladium-catalyzed coupling reaction of acid chlorides with organotins. J Org Chem 1983;48:4634–42, http://pubs.acs.org/doi/abs/10.1021/jo00172a038.
[27] Sieber F, Wentworth PJ, Janda KD. Exploring the scope of poly(ethylene glycol) (PEG) as a soluble polymer matrix for the stille cross-coupling reaction. J Comb Chem 1999;1:540–6, http://pubs.acs.org/doi/abs/10.1021/cc990052o.
[28] Hou Q, Xu Y, Yang W, Yuan M, Peng J, Cao Y. Novel red-emitting fluorene-based copolymers. J Mater Chem 2002;12:2887–92, http://pubs.rsc.org/en/Content/ArticleLanding/2002/JM/b203862e.
[29] Lu P, Zhang HQ, Shen FZ, Yang B, Li D, Ma YG, et al. A wide-bandgap semiconducting polymer for ultraviolet and blue light emitting diodes. Macromol Chem Phys 2003;204:2274–80, http://onlinelibrary.wiley.com/doi/10.1002/macp.200300006/abstract.
[30] Lu P, Zhang HQ, Li M, Zheng Y, Ma YG, Chen XF, et al. Photophysical properties of fluorene-based copolymers synthesized by connecting twisted biphenyl units with fluorene via para- and meta-linkages. Polym Int 2008;57:987–94, http://onlinelibrary.wiley.com/doi/10.1002/pi.2436/abstract.
[31] Walczak RM, Brookins RN, Savage AM, Aa EM, Reynolds JR. Convenient synthesis of functional polyfluorenes via a modified one-pot suzuki–miyaura condensation reaction. Macromolecules 2009;42:1445–7, http://pubs.acs.org/doi/abs/10.1021/ma802462v.
[32] Ishiyama T, Murata M, Miyaura N. Palladium(0)-catalyzed cross-coupling reaction of alkoxydiboron with haloarenes: a direct procedure for arylboronic esters. J Org Chem 1995;60:7508–10, http://pubs.acs.org/doi/abs/10.1021/jo00128a024.
[33] Benmansour H, Shioya T, Sato Y, Bazan GC. Anthracene-containing binaphthol chromophores for light-emitting diode (LED) fabrication. Adv Funct Mater 2003;13:883–6, http://onlinelibrary.wiley.com/doi/10.1002/adfm.200304456/abstract.
[34] Hou Q, Zhou QM, Zhang Y, Yang W, Yang RQ, Cao Y. Synthesis and electroluminescent properties of high-efficiency saturated red emitter based on copolymers from fluorene and 4,7-di(4-hexylthien-2-yl)-2,1,3-benzothiadiazole. Macromolecules 2004;37:6299–305, http://pubs.acs.org/doi/abs/10.1021/ma049204g.
[35] Yang RQ, Tian RY, Yan JG, Zhang Y, Yang J, Hou Q, et al. Deep-red electroluminescent polymers: synthesis and characterization of new low-band-gap conjugated copolymers for light-emitting diodes and photovoltaic devices. Macromolecules 2005;38:244–53, http://pubs.acs.org/doi/abs/10.1021/ma047969i.
[36] Thomas KRJ, Lin JT, Velusamy M, Tao YT, Chuen CH. Color tuning in benzo[1,2,5]thiadiazole-based small molecules by amino conjugation/deconjugation: bright red-light-emitting diodes. Adv Funct Mater 2004;14:83–90, http://onlinelibrary.wiley.com/doi/10.1002/adfm.200304486/abstract.
[37] Reichardt C. Solvatochromic dyes as solvent polarity indicators. Chem Rev 1994;94:2319–58, http://pubs.acs.org/doi/abs/10.1021/cr00032a005.
[38] Xie ZQ, Xie WJ, Li F, Liu LL, Wang H, Ma YG. Controlling supramolecular microstructure to realize highly efficient nondoped deep blue organic light-emitting devices: the role of diphenyl substituents in distyrylbenzene derivatives. J Phys Chem C 2008;112:9066–71, http://pubs.acs.org/doi/abs/10.1021/jp801033j.
[39] Hu DH, Lu P, Wang CL, Liu H, Wang H, Wang ZM, et al. Silane coupling dicarbazoles with high triplet energy as host materials for highly efficient blue phosphorescent devices. J Mater Chem 2009;19:6143–8, http://pubs.rsc.org/en/Content/ArticleLanding/2009/JM/b906782e.
[40] Yang JL, Yan DH. Weak epitaxy growth of organic semiconductor thin films. Chem Soc Rev 2009;38:2634–45, http://pubs.rsc.org/en/Content/ArticleLanding/2009/CS/b815723p.
[41] Gutierrez MCG, Linares A, Hernandez JJ, Rueda DR, Ezquerra TA, Poza P, et al. Confinement-induced one-dimensional ferroelectric polymer arrays. Nano Lett 2010;10:1472–6, http://pubs.acs.org/doi/abs/10.1021/nl100429u.